

# Self-assembly of iron platinum based nanoparticles on diethylene glycol and carbon-coated copper grid substrates

P Sarmphim <sup>1</sup>, K Chokprasombat <sup>2</sup>, Y Sirisathitkul <sup>3</sup> and C Sirisathitkul <sup>4\*</sup>

<sup>1</sup> Department of General Education, Faculty of Liberal Arts, Rajamangala University of Technology Srivijaya, Songkhla, Thailand

<sup>2</sup> Department of Physics, Faculty of Science, Thaksin University, Phatthalung, Thailand

<sup>3</sup> School of Informatics, Walailak University, Nakhon Si Thammarat, Thailand

<sup>4</sup> Center of Excellence in Functional Materials and Nanotechnology, School of Science, Walailak University, Nakhon Si Thammarat, Thailand

\* Corresponding author E-mail address: [chitnarong.siri@gmail.com](mailto:chitnarong.siri@gmail.com)

**Abstract.** Self-assembly of magnetic nanoparticles into a long-range monolayer pattern is under investigation in both theoretical aspect and data storage application. In this work, the effect of liquid and solid substrates on the nanoparticle assembly was compared. Iron (III) dibenzoylmethane ( $\text{Fe}(\text{dbm})_3$ ) was used as an alternative reagent to highly toxic iron pentacarbonyl ( $\text{Fe}(\text{CO})_5$ ) in the co-reduction with platinum acetylacetonate ( $\text{Pt}(\text{acac})_2$ ). The as-synthesized iron-platinum (FePt) based nanoparticles were dropped either on diethylene glycol (DEG) or directly on carbon-coated copper grid. In the case of DEG, the drastic movement of nanoparticles during the liquid-air interface assembly tracked by a camera terminated after 15 seconds. A subsequent inspection after transferring the monolayers from DEG to carbon-coated copper grid substrates confirmed the extended area of ordered nanoparticles from the liquid-air interface assembly. These results demonstrated that the liquid-air interface method is effective not only in patterning monodisperse nanoparticles but also those with wider size distributions.

## 1. Introduction

Iron-platinum (FePt) nanoparticles have either disordered face centered cubic (fcc) structure or ordered face centered tetragonal (fct). The  $L1_0$  FePt with the fct structure may be obtained from the direct chemical synthesis or be converted from the fcc phase by the high temperature annealing [1]. Other FePt based nanoparticles can also be obtained with variations in elemental ratios, such as  $L1_2$   $\text{Fe}_3\text{Pt}$  and  $L1_2$   $\text{FePt}_3$ . The  $L1_2$   $\text{FePt}_3$  is antiferromagnetic whereas the  $L1_0$  FePt and  $L1_2$   $\text{Fe}_3\text{Pt}$  are ferromagnetic [2]. The ferromagnetic FePt and  $\text{Fe}_3\text{Pt}$  have potential implementations as ultrahigh density recording media and nanostructured permanent magnets. Applications in ultrahigh density recording and sensing require homogeneous arrangements of nanoparticles. Self-assembly is a facile technique to produce a long-range ordered pattern without complicated steps demanded in lithography processes [3]. In addition to direct dropping on solid substrates, self-assembly at liquid-air interface is an alternative using the drop-casting nanoparticle suspension on the surface of liquid. A monolayer of

assembled nanoparticles, referred to as Langmuir film, is formed and can subsequently be transferred to a solid substrate in a lift-off process [4].

In this work, the green synthesis using an alternative reagent to highly toxic  $\text{Fe}(\text{CO})_5$  was implemented and resulting FePt based nanoparticles were assembled. Since the variations in size and shape severely affect the nanoparticle arrangements, nanoparticles were analyzed by transmission electron microscope (TEM) image processing and the types of substrates were investigated to promote the long-range order of nanoparticle assembly.

## 2. Experimental

FePt based nanoparticles were synthesized from the reaction between iron (III) dibenzoylmethane ( $\text{Fe}(\text{dbm})_3$ ) and platinum acetylacetonate ( $\text{Pt}(\text{acac})_2$ ) as detailed in [5]. Self-assembly of nanoparticles was compared between on solid substrates and at liquid-air interface. Carbon-coated copper TEM grid substrate, used as the solid substrate, was firstly inspected by an optical microscope before direct dropping of nanoparticle suspensions using a micropipette. In the liquid-air interface method, nanosuspensions were dropped on diethylene glycol (DEG) surface. The floating Langmuir film, visible to unaided eyes, was tracked by using a CCD camera (PixeLink PL-B771F) for 20 s. To collect nanoparticle assembly for TEM imaging, each carbon-coated copper grid substrate was placed under the Langmuir film and then slowly lifted-off. Images of dried nanoparticles on carbon-coated copper grid substrates were obtained by the 200 kV TEM (JEOL JEM-2010). The size of nanoparticles in TEM images was analyzed by the image processing procedure described in [6].

## 3. Results and discussion

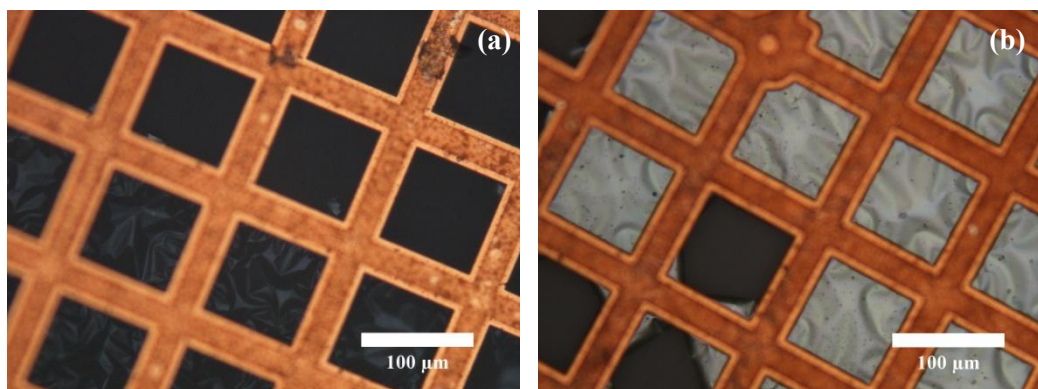


**Figure 1.** Optical micrographs of TEM grid substrate (a) before and (b) after the direct dropping of nanoparticle suspension.

Carbon-coated copper TEM grid substrates are 3 mm in diameter with 200 mesh. Square films with area of  $0.11 \text{ mm}^2$  can be inspected under the microscope. For empty grids in figure 1(a), the majority of the films are flat but they are not entirely smooth. Moreover, some films are torn. Such defect inevitably affects the nanoparticle assembly but can be spotted during the microscope scan. After dropping of nanosuspensions, the substrates in figure 1(b) are covered by layers of nanoparticles with exclusion of some films.

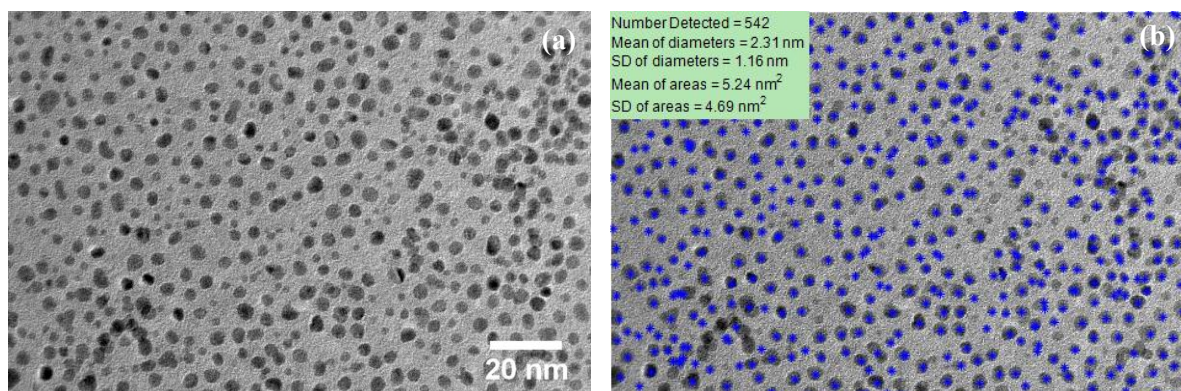


**Figure 2.** Example of TEM images of nanoparticles (a) before and (b) after the imaging processing.

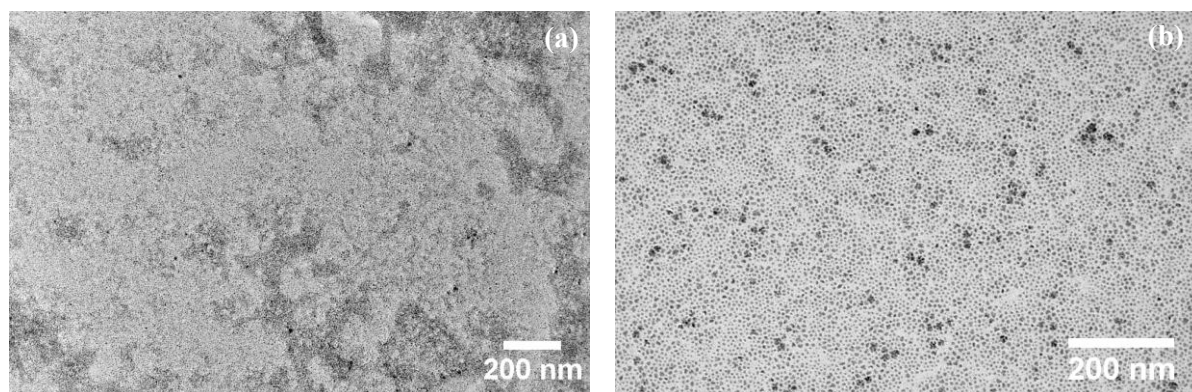
**Table 1.** Size analysis results by the image processing on 5 TEM images.

Image Number	Number of detected nanoparticles	Mean of area (nm <sup>2</sup> )	Mean diameter (nm)	SD of diameter (nm)
1	564	6.14	2.47	1.32
2	542	5.24	2.31	1.16
3	635	7.09	2.65	1.41
4	672	5.93	2.44	1.26
5	649	6.63	2.59	1.31

The Fe:Pt atomic ratio of nanoparticles was averaged from EDS measurements as 0.57:1. The FePt<sub>3</sub> phase was identified by XRD [5]. The size and shape of nanoparticles are demonstrated in figure 2(a). Despite some variations in morphology, most FePt based nanoparticles can be approximated as spheres. Image processing was performed on TEM images exemplified in figure 2(b) and the results from 5 images are summarized in table 1. The advantage of image processing technique over the traditional one-by-one inspection is apparent from a large numbers of particles analyzed in each image. A sampling size over 3000 increases the accuracy of the analysis. Interestingly, the numbers of detected nanoparticles in all 5 images are comparable, suggesting the even spatial distribution. The mean diameter is varied from 2.31 to 2.65 nm. However, the standard deviations as high as 1.41 indicate the polydispersity of nanoparticles.

Figure 3 demonstrates the effect of the substrate on the self-assembly of nanoparticles. The direct dropping on the carbon-coated copper grid substrate results in uneven spatial distribution of nanoparticles in figure 3(a). Moreover, the nanoparticle stacking occurs in some area due to the attractive van der Waals force and magnetic dipole interaction among the ferromagnetic nanoparticles. By contrast, nanoparticles are evenly distributed in a larger area in figure 3(b). By tracking the floating Langmuir film by a CCD camera, the movement was virtually terminated around 15 s after the liquid-air interface assembly. Since the FePt based nanoparticles are covered with surfactants that have polar head and non-polar tail, the mechanisms are the floating of hydrophobic tail and the absorption of hydrophilic head of ligand-capped nanoparticle at the liquid-air interface. The stability of spherical nanoparticle is related to the binding energy of individual nanoparticles at liquid-air interface. Estimated by Pieranski's model [7], the binding energy is mainly proportional to the surface tension coefficient of the liquid subphase. Since the surface tension of DEG is lower than those of water and ethylene glycol, DEG is appropriate subphase for stabilizing surface-modified nanoparticle in the assembly process.

Compared to the liquid-air interface self-assembly of FePt nanoparticles by Dong et al. [8], there are more irregularity and defects in our pattern. This is largely attributed to the variation in nanoparticle size. Nevertheless, our results support the work by Bigioni et al. [9] that not only monodisperse nanoparticles but polydisperse nanoparticles can also be self-assembled over an extended area by the liquid-air interface method. The mechanism during the solvent evaporation illustrated in [9] regulates the final pattern.



**Figure 3.** Comparison between the nanoparticle assemblies obtained from (a) direct dropping and (b) liquid-air interface method.

#### 4. Conclusions

TEM image processing indicated a variation in size of nanoparticles synthesized from the reaction between  $\text{Fe}(\text{dbm})_3$  and  $\text{Pt}(\text{acac})_2$ . It followed that self-assembly of these magnetic nanoparticles into a long-range monolayer pattern was not obtained by the direct dropping on solid substrates. However, it was demonstrated that these polydisperse nanoparticles could be self-assembled into a monolayer over an extended area of DEG surface. This self-assembly at the liquid-air interface therefore provides the simple but effective pathway in patterning nanostructures.

**Acknowledgments** The authors would like to thank P. Harding of Department of Chemistry, Walailak University for her suggestions. The technical assistance in TEM imaging by P. Pinsrithong of Scientific Equipment Center, Prince of Songkla University is acknowledged.

#### References

- [1] Tzitzios V, Basina G, Colak L, Niarchos D and Hadjipanayis G 2011 *J. Appl. Phys.* **109** 07A718
- [2] Chen S and Andre P 2012 *Int. J. Nanotechnol.* **9** 39–68
- [3] Neouze M-A 2013 *J. Mater.Sci* **48** 7321–49
- [4] Giner-Casares J J, Brezesinski G and Möhwald H 2014 *Curr. Opin. Colloid Interface Sci.* **19** 176–82
- [5] Sarmphim P, Chokprasombat K, Sirisathitkul C, Sirisathitkul Y, Ratchaphonsaenwong K, Pinitsoontorn S and Harding P 2016 *J. Clust. Sci.* **27** 1–8
- [6] Chokprasombat K, Sirisathitkul Y, Sirisathitkul C, Sarmphim P and Harding P 2015 *J. Supercond. Nov. Magn.* **28** 1199–206
- [7] McGorty R, Fung J, Kaz D and Manoharan V N 2010 *Mater. Today* **13** 34–42
- [8] Dong A, Chen J, P. M. Vera P M, J. M. Kikkawa J M and Murray C B 2010 *Nature* **466** 474–7
- [9] Bigioni T P, Lin X-M, Nguyen T T, Corwin E I, Whitten T A and Jaeger H 2006 *Nature Mater.* **28** 265–70